Curing Processes in Solvent-Borne Alkyd Coatings with Different Drier Combinations

S. J. F. Erich,[†] L. G. J. van der Ven,*[,‡] H. P. Huinink,[†] L. Pel,*[,†] and K. Kopinga[†]

Department of Applied Physics, Eindhoven University of Technology, P.O. Box 513, 5600 MB Eindhoven, The Netherlands, and Akzo Nobel Coatings Research Arnhem, P.O. Box 9300, 6800 SB Arnhem, The Netherlands

Received: December 8, 2005; In Final Form: March 8, 2006

The concern regarding the effect of chemicals on the environment has increased considerably in recent years. Nowadays, technological developments in the coating industry are largely influenced by environmental issues and subsequent legislation. One of these issues is the tendency to replace cobalt as a catalyst with more environmentally friendly alternatives, because studies have indicated possible carcinogenicity. Not much knowledge is available on the effects of catalysts (driers) on the in-depth drying of alkyd coatings. Therefore we have studied the effect of cobalt as a primary drier combined with Ca and Zr as secondary driers on the in-depth curing of high solid solvent-borne alkyds. The profiling of the curing of alkyd coatings is performed with a new high-spatial-resolution NMR setup. In this study, two effects observed in the solvent-borne alkyd coatings are investigated. One is that when Ca and Zr are added as secondary driers the speed of the observed cross-linking front increases. Second, in the deeper un-cross-linked region below the front, the signal of the NMR profiles was found to decrease proportional to $\sqrt{t}$. This could be explained by the presence of slowly reacting species that diffuse into the deeper uncured region of the coating, after which they cross-link. The model describing the effect of these reactive species also indicates that the signal decrease is inversely proportional to coating thickness L, which was confirmed by additional measurements.

1. Introduction

Coatings can be found everywhere, e.g., on furniture, cars, airplanes, and buildings. An important class of coatings are the ones based on alkyd resins. In 1996 the European coating industry consumed 1.8 million tonnes of binders for the production of paints, of which 25% were alkyds.[1] The curing of alkyd coatings is a complex autoxidation process.[2−5] By the addition of so-called driers this process can be accelerated considerably. Cobalt is the most commonly used drier in commercial alkyd paints. In most commercially available coatings secondary driers (Ca and Zr) are added to Co to enhance the oxidation. In the literature various statements circulate about the effects of the addition of Ca and Zr.[6−11] As an example, Zr is said to improve the through-drying, i.e., drying in the deeper layers of the coating. Up until now, however, the knowledge on the effects of driers on the in-depth drying of coatings has been still rather limited. In this paper we will focus on the effects of Ca/Zr as secondary driers on the in-depth drying of solvent-borne alkyd coatings.

Only a few analytical techniques are available that can probe the coating structure as a function of time. One of these techniques is confocal Raman microscopy (CRM), in which the chemical changes can be probed locally, e.g., the change in double bonds.[12−17] In this study we use a high-spatial-resolution NMR setup. This setup has the ability to probe in a noninvasive way nontransparent coating systems with a spatial resolution of 5 μm.[18] The NMR setup measures the hydrogen density profiles and the local mobility of the hydrogen nuclei inside the coating by probing the signal decay. During the drying process the mobility decreases and the signal decay increases, allowing the drying process to be visualized.

In section 2 we first review the drying process of alkyd resins and the effects of driers on this process. In the following section, the materials and methods are further explained. The measurements will be discussed in section 4. In section 5 we introduce a model to explain in more detail the measurements in which drying in deeper regions of the coating is observed. Finally we end with the discussion and conclusions.

2. Drying of Alkyd Coatings

The drying process of an alkyd coating can be divided into two stages. The first stage is a physical drying stage in which the solvent evaporates. The second stage is a curing stage (chemical or oxidative drying) in which the resin of the coating reacts and forms a network. These two stages involve different time scales; the evaporation stage takes minutes to several hours, whereas the curing process takes place over several hours to days or even months. This last stage can continue slowly for years. In this paper we will focus on the second stage, the curing stage.

The curing of alkyd coatings is a lipid autoxidation process.[2−5,19−23] Autoxidation is generally divided into six stages.[24] The stages that are distinguished are the induction period, the initiation, hydroperoxide formation, and decomposition, followed by cross-linking and degradation. Many possible intermediate and final species can be found during this complex autoxidation process.[3,5]

The autoxidation process is a slow process, and driers are needed to increase the speed of this process.[24] These driers enhance the decomposition and/or formation of the hydroper-

* Authors to whom correspondence should be addressed. E-mail: leo.vanderven@akzonobel.com; l.pel@tue.nl.
[†] Eindhoven University of Technology,
[‡] Akzo Nobel.

10.1021/jp057148v CCC: $30.25
Published on Web 03/30/2006

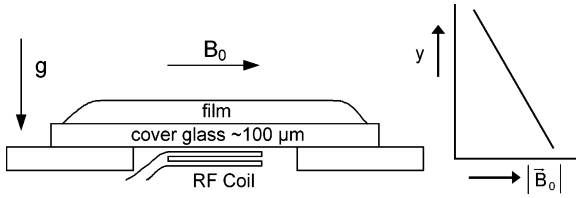

Figure 1. Schematic representation of the RF coil and film placement inside the magnet. The right graph shows the variation of the magnetic field as a function of position inside the coating. Because of this gradient (36 T/m) a resolution of 5 μm in the vertical direction can be achieved.

oxides, finally resulting in an increased amount of radicals. In general, drier metals are divided into two categories:[6−8,10,11] primary driers (active driers) and secondary driers (through driers). The first group, the primary driers (in this paper this group is referred to as the catalyst), is said to promote rapid surface drying with limited through-drying properties. Cobalt, manganese, and iron belong to this group. The second group, the secondary or auxiliary driers, is assumed to have two effects; they are said to increase the stability of the primary drier and promote the through-drying. Many different effects have been reported for many different driers and drier combinations and concentrations in model systems.[8,9,25] In a paper by Mallegol et al.[9] the influence of drier combinations on the through-drying in water-borne alkyd emulsions was investigated by analyzing the T_2 relaxation times obtained using an NMR profiling setup. They concluded that more uniform cross-linking is achieved using a combination of Co, Ca, and Zr. In this paper the dynamics of the curing process will be studied in more detail.

3. Materials and Methods

3.1. Materials. The high solid solvent-borne alkyd resin used has a solid content of about 80% and a oil length of 79%. The cobalt concentration used was 0.06% mass/mass with respect to the solid content. The concentration of Ca was 0.23% mass/mass, and that of Zr was 0.38% mass/mass when added. The coatings were supplied by Akzo Nobel. The coatings were applied on a microscope cover glass using a 150 μm spiral application rod, resulting in a dry film thickness of about 90 μm.

3.2. NMR Setup. A high-resolution NMR setup is used for profiling the curing of the coatings. The working principle of this setup is based on the fact that magnetic nuclei located in a magnetic field can be selectively excited by a radio frequency (RF) pulse. The resonance frequency (f) depends linearly on the applied magnetic field (B), $f = \gamma|B|$, with γ the gyromagnetic ratio (for hydrogen nuclei, $\gamma = 42.58$ MHz/T). To obtain a high spatial resolution (<10 μm) a very high magnetic field gradient should be applied. To achieve this the magnitude, the magnetic field is varied with position, $f = \gamma(|\vec{B}| + Gy)$, where $G = \partial|\vec{B}|/\partial y$, according to the GARField design introduced by Glover et al.[18] The sample can be placed directly on top of a surface coil, as shown in Figure 1, which gives a good signal-to-noise ratio. Also the gravity is perpendicular to the applied paint film, which makes it possible to measure wet films. In our study we use an NMR setup that contains an electromagnet generating a magnetic field of 1.4 T at the position of the sample. The gradient is 36.4 ± 0.2 T/m.

The NMR pulse sequence used to obtain the hydrogen density profiles and the signal decay is an Ostroff−Waugh[26] sequence ($90°_x-\tau-[90°_y-\tau-\text{echo}-\tau]_n$). The interecho time ($2\tau$) was set to 200 μs. From the signal decay acquired by this pulse sequence several T_2 relaxation times can be obtained, depending on the average local mobility.[27]

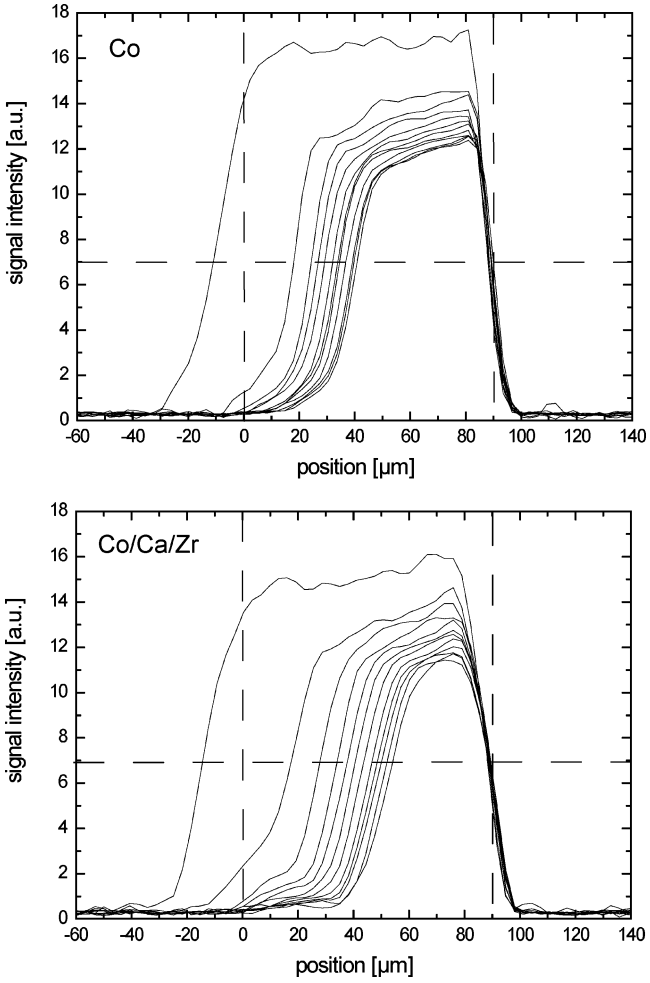

Figure 2. NMR signal intensity measured as a function of position inside the coating at different times, for both Co and Co/Ca/Zr as a catalyst. The glass plate is located at the right side of the coating, indicated by the right vertical dashed line. The left dashed line shows the top of the coating. In both graphs the first profile is given during the evaporation of the solvent, $t = 0.6$ h. The second profile in both graphs is plotted for $t = 5.6$ h and then every 6.3 h. The point of intersection of horizontal dashed line with the left side of the profiles is taken as the position of the front.

4. Results

4.1. Profiles. In Figure 2 profiles of the alkyd coatings for both Co and Co/Ca/Zr as driers are shown. The profiles were acquired approximately every 20 min; however, only several representative profiles, after smoothing over all profiles to reduce the noise, are plotted. The first profile shows the coating after 0.6 h, during the evaporation stage. The left vertical dashed line indicates the position of the surface of the coating after the evaporation of the solvent. The right vertical dashed line indicates the location of the cover glass sheet on which the coating was cast. After the evaporation stage a front forms and moves downward to the bottom of the coating. In previous work we have shown that this front is a cross-linking front.[27,28] Figure 2 clearly shows the formation of a front. Another interesting observation that can be made in this figure is the decrease of the NMR signal in the region where the curing front has not yet passed. This observation will be discussed in section 4.3, but first we will focus on the formation and behavior of the curing front.

4.2. Drying Front. In a recent paper we confirmed that an oxygen gradient is present, and as a result of this gradient we observed a cross-linking front.[28] This front, resulting in a skin

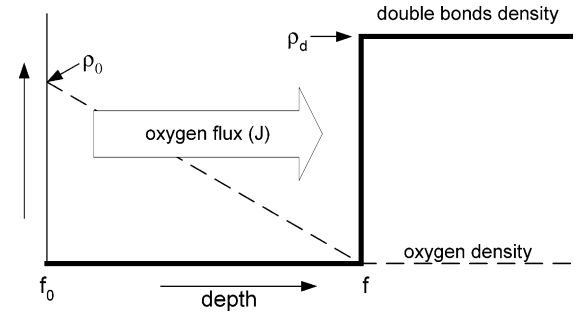

Figure 3. Schematic representation of the drying model. The dashed line indicates the oxygen density. The black line indicates the amount of double bonds. Because of the high reaction rate the oxygen density is taken to be zero at the front.

layer, was observed in water-borne alkyd emulsions, solvent-borne alkyds, and high solid solvent-borne alkyds, only when cobalt was used as a catalyst. The diffusion of oxygen together with a high reaction rate is the basis of the formation and movement of the front. Whenever cross-linking occurs, the NMR signal decay is so fast that part of the signal is already lost at the moment of the acquisition of the profile, making the front visible in the NMR profiles.[27] The formation of this skin layer is schematically depicted in Figure 3. At the surface the oxygen concentration is constant, and the oxygen diffuses and is consumed at the cross-linking front to form a network. It is assumed that the oxygen reacts instantaneously, causing the front to move toward the coating substrate. This behavior can be described by the following equation[28]

$$f(t) = f_0 + \sqrt{2\nu D\rho_0(t - t_0)} \qquad (1)$$

where D (m^2/s) is the diffusion constant of oxygen in the coating, ρ_0 (mol/m^3) the oxygen density in the surface layer of the coating film, and ν (m^3/mol) the cross-linked volume per mole of oxygen.

In Figure 4 the front position is plotted squared against time, which according to eq 1 should result in straight lines. The front positions are determined from the intersection of the horizontal dashed line in Figure 2 with the front. The horizontal dashed line is positioned arbitrarily at approximately half of the height of the front. Figure 4 shows that the front movement is faster when Ca and Zr are present next to Co. Within the model the change in front speed can only be explained from the three parameters in eq 1, the oxygen solubility ρ_0, the oxygen diffusion D, or the cross-linked volume per mole of oxygen ν. If the network structure changes, then the amount of oxygen per cross-linked volume (ν) is expected to change. To check whether the network of both coatings differs, the glass transition temperature was determined after the coatings were fully cured. The glass transition (T_g) was found to be the same within the experimental error (13 ± 2 °C and 11 ± 2°C for Co and Co/Ca/Zr, respectively). From this observation it can be expected that no significant differences in the network structure are present, meaning no change in ν is expected. Then the other two possibilities remain, which are a change in oxygen solubility at the surface of the coating or a change of the diffusion of oxygen. Further investigations are necessary to clarify this point.

4.3. Curing in Deeper Regions of the Coating. From the NMR profiles in Figure 2 we have noticed that the signal decreases in the deeper un-cross-linked regions below the cross-linking front. This decrease is small and occurs fairly homogeneously at the substrate side of the front. Plots of the signal intensity in this region against the square root of time result in

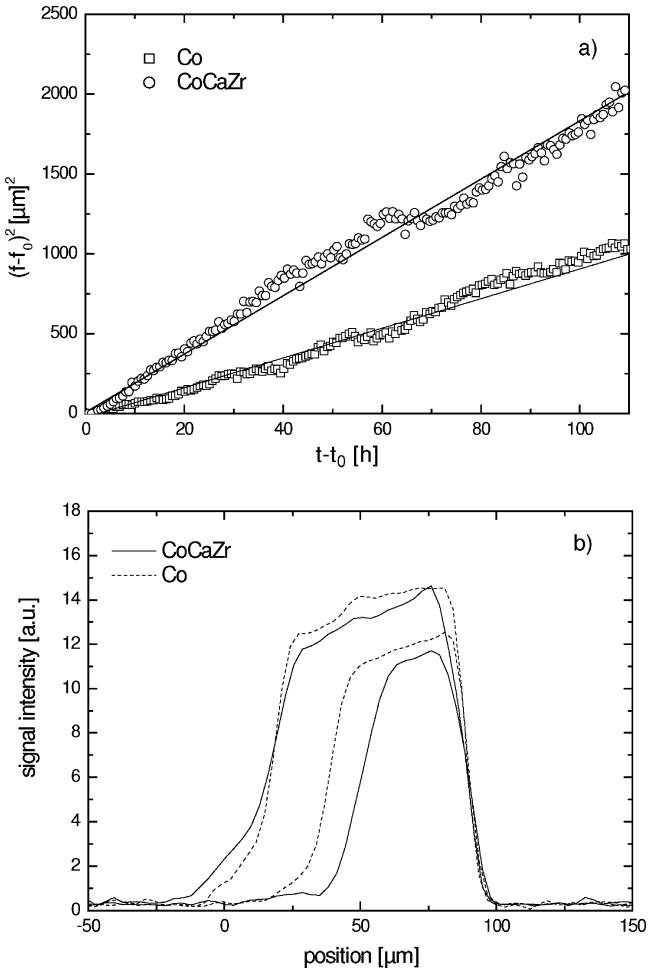

Figure 4. (a) Squared front position plotted as a function of time for both Co and Co/Ca/Zr as driers. (b) NMR profiles of a coating with Co and a coating with Co/Ca/Zr as driers at 6 and 60 h after application. Both figures indicate a faster front movement for the Co/Ca/Zr combination.

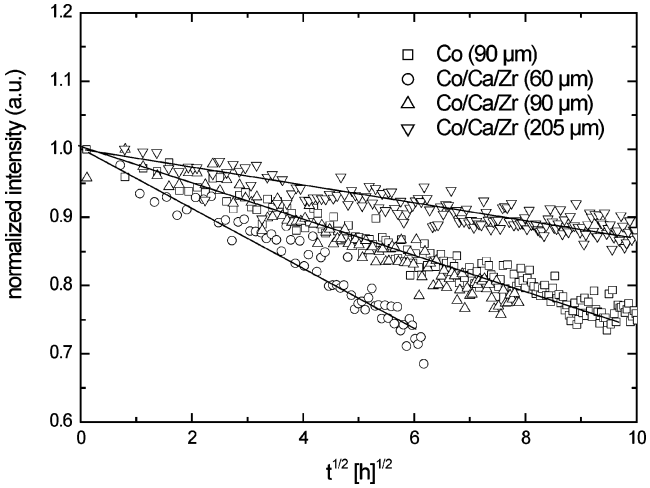

Figure 5. Normalized NMR signal in the deeper region of the coating as a function of the square root of the curing time. Note that the NMR signal intensity decreases faster for thinner coatings. For both drier combinations (Co and Co/Ca/Zr) with a similar coating thickness the signal intensity decreases at the same rate.

straight lines; see Figure 5. Note that the signal intensity is normalized to be able to compare different samples. The signal intensity is only plotted for one position in the deeper regions of the coating; however, the observed behavior applies to the

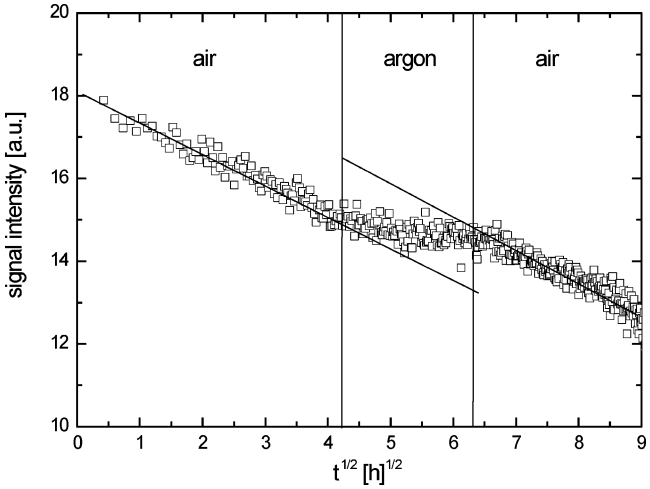

Figure 6. Normalized NMR signal in the deeper region of the coating as a function of the square root of the curing time. While the argon atmosphere is applied the signal decrease stops.

whole un-cross-linked region. Additionally, the results for the samples with or without Ca and Zr show no difference in signal decrease. There are two possible explanations for a signal decrease proportional to $\sqrt{t}$. One is that remaining solvent is slowly evaporating from the coating or, second, somehow cross-linking in the deeper regions takes place. First, let us consider the first explanation. When the thickness of the skin layer increases, it blocks the evaporation of the solvent by the increased resistance of this cross-linked layer. Because the thickness of this resistive layer increases with $\sqrt{t}$, the rate of solvent loss decreases with $\sqrt{t}$. Integration results in a solvent loss (and thus signal decrease) proportional to $\sqrt{t}$. If we would stop the front movement and let the evaporation continue, then the signal from the deeper regions would continue to decrease. Because now the thickness of the cross-linked layer would stop increasing, a signal decrease faster than $\sqrt{t}$ would occur. In a previous measurement on a solvent-borne alkyd the front movement was stopped by replacing the oxygen with a dry argon atmosphere around the coating.[28] In that experiment the signal in the deeper layers also showed a $\sqrt{t}$ behavior; see Figure 6. At $t = 16$ h the argon atmosphere was created and the signal decrease stops; after restoring the air atmosphere the signal in the deeper layers decreases again. A signal decrease faster than $\sqrt{t}$ is not observed, but instead the signal decrease stops, ruling out this explanation. The second explanation, based on the diffusion of reactive species into the deeper regions, remains. This possibility is investigated in the next section.

5. Model

As has been shown in the previous section, cross-linking in the deeper regions is related to the oxygen flux, because removal of the oxygen supply above the coating stops the signal decrease. Therefore we assume that the flux of oxygen partially results in fast moving reactive species (high diffusion). These species are slowly reacting, resulting in a homogeneous distribution. The production of these reactive species is equal to c_1J, where c_1 is the fraction of the oxygen influx that is used to create these species. The following differential equation describes the density ρ_r of these species

$$\frac{\partial \rho_r}{\partial t} = \frac{c_1 J}{L} - k\rho_r \qquad (2)$$

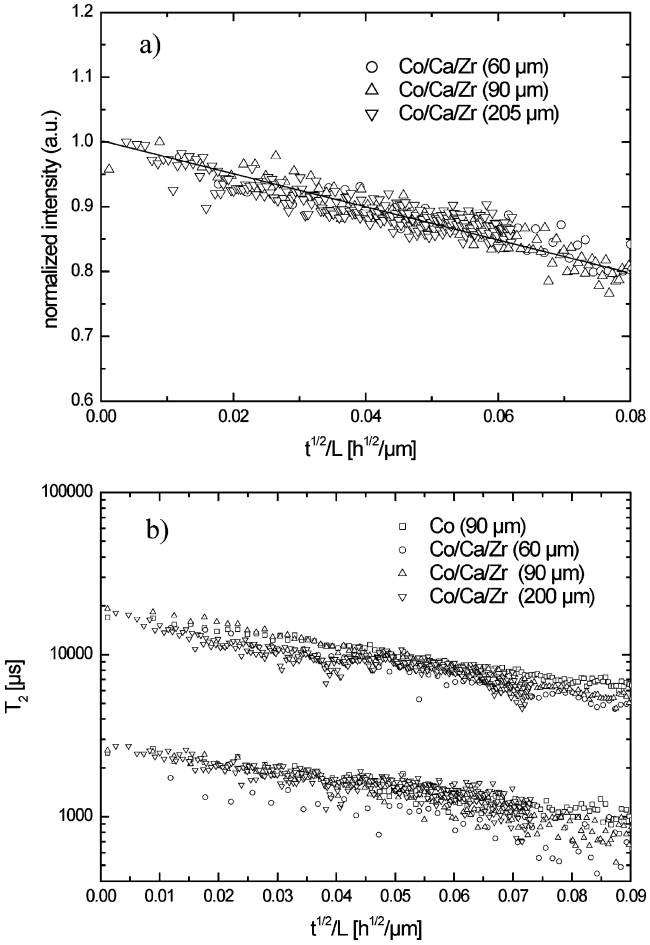

Figure 7. (a) Normalized NMR signal intensity as a function of $\sqrt{t}/L$ for the Co/Ca/Zr drier combinations for three different coating thicknesses. (b) Two T_2 relaxation times obtained from the signal decay as a function of $\sqrt{t}/L$ for the different drier combinations and coating thicknesses. Both figures indicate that the same scaling law applies.

where J is the oxygen flux, L the thickness of the coating, and k the reaction constant for these species. By insertion of the equation for the oxygen flux $J = D\rho_0/f(t)$,[28] where $f(t)$ is defined by eq 1 with $f(0) = 0$ and $t_0 = 0$, the following equation is obtained

$$\frac{\partial \rho_r}{\partial t} = \frac{c_1}{L}\sqrt{\frac{\rho_o D}{2\nu t}} - k\rho_r \qquad (3)$$

To allow the slowly reactive species to distribute homogeneously, the reaction time should be much higher than the diffusion time, $\tau_r/\tau_D = D/L^2k \gg 1$. From the experiment shown in Figure 6, the time to stop the signal decrease can be estimated to be about half an hour, which means that k is on the order of 10^{-3} s^{-1}. Taking typical constants for the thickness this means $D > L^2k = (10^{-4})^2 10^{-3} = 10^{-11}$ m^2/s, which is reasonable for the diffusion constant of these reactive species in the un-cross-linked area. Whether this condition holds in the cross-linked area is unclear. At the start of the curing process the production of reactive species is high, and eq 3 is governed by the first term at the right-hand side. From this equation it can be derived that initially $(\partial\rho_r/\partial t)/\rho_r$ varies with t^{-1}, meaning that the relative contribution of $\partial\rho_r/\partial t$ decreases. Finally, at sufficiently long times a steady-state situation develops, and eq 3 can then be approximated by

$$k\rho_r = \frac{c_1}{L}\sqrt{\frac{\rho_0 D}{2\nu t}} \tag{4}$$

Now we assume that the signal decreases proportionally to the reaction rate of the species. This assumption is based on the idea that when such a species reacts and forms a cross-link the mobility of the surrounding hydrogens decreases dramatically, reducing their contribution to the NMR signal. This results in the following equation for the signal loss

$$\frac{dS(t)}{dt} = -\chi k\rho_r = -\frac{\chi c_1}{L}\sqrt{\frac{\rho_0 D}{2\nu t}} \tag{5}$$

where χ is the proportionality constant between the signal decrease and the amount of reactions that have occurred. Starting from a signal $S(0)$ the following equation is obtained

$$S(t) = S(0) - \frac{\chi c_1}{L}\sqrt{\frac{2\rho_0 D}{\nu}}t = S(0) - \frac{\chi c_1}{\nu L}f(t) \tag{6}$$

This equation indicates that the signal decay in the deeper region of the coating proceeds faster in thinner coatings. The model predicts that the time is scalable with L^{-1}, which is supported by the experimental data plotted in Figure 7a. When the T_2 relaxation times obtained from the signal decay in the deeper regions for all measured coatings are plotted against $\sqrt{t}/L$, they show a similar behavior (Figure 7b).

The present model correctly explains the signal decrease with $\sqrt{t}$ and has correctly predicted its dependence on the coating thickness. Therefore we conclude that the diffusion of reactive species is the origin of the observed effects. The fact that this phenomenon is only observed in solvent-borne systems and not in water-borne alkyd emulsions[27] can also be explained by the diffusion of the reactive species. The diffusion is restricted in water-borne systems, which have a viscosity that is substantially higher than that of solvent-borne systems after evaporation of the water or solvent.

6. Conclusions and Discussion

We have observed that the addition of Ca/Zr as secondary driers, next to Co as a primary drier, results in an increased speed of the curing front. Also a signal decrease in the deeper regions of the coating proportional to $\sqrt{t}$ was observed. Addition of of Ca and Zr did not change the signal decrease in the deeper regions of the coating. Contrary to statements in the literature, we do not observe a speedup of the through-drying by the addition of Ca and Zr;[6−8,10,11] only faster growth of the skin layer is observed. Two probable explanations for the signal decrease in the deeper regions were investigated. One explanation based on the evaporation of the remaining solvent was rejected, based on additional experiments. The other explanation was based on the diffusion of less reactive species. The low reactivity of these species allows penetration in the deeper regions of the coating; after which they react and cross-link. A model describing this process correctly predicts the observed $\sqrt{t}$ behavior of the signal decrease. This model also predicts that the signal decrease scales inversely with the thickness of the coating (L). The scaling with $\sqrt{t}/L$ was experimentally confirmed by changing the coating thickness.

Acknowledgment. A part of this research is supported by the Center for Building and Systems TNO-TU/e. We thank Akzo Nobel for supplying the high solid solvent-borne alkyd systems.

References and Notes

(1) *A Profile of the European Paint Industry*, 12th ed.; Information Research Limited: London, 1998.
(2) Porter, N. A.; Weber, B. A.; Weenen, H.; Khan, J. A. *J. Am. Chem. Soc.* **1980**, 5597.
(3) Porter, N. A.; Lehman, S.; Weber, B. A.; Smith, K. J. *J. Am. Chem. Soc.* **1981**, *103*, 6447−6455.
(4) Porter, N. A.; Mills, K. A.; Carter, R. L. *J. Am. Chem. Soc.* **1994**, *116*, 6690−6696.
(5) Porter, N. A.; Wujek, D. G. *J. Am. Chem. Soc.* **1984**, *106*, 2626−2629.
(6) Bieleman, J. H. *Additives for Coatings*; Wiley-VCH: Weinheim, 2000.
(7) Meneghetti, S. M. P.; de Souza, R. F.; Monteiro, A. L.; de Souza, M. O. *Prog. Org. Coat.* **1998**, *33*, 219−224.
(8) Bieleman, J. H. *Macromol. Symp.* **2002**, *187*, 811−821.
(9) Mallegol, J.; Barry, A. M.; Ciampi, E.; Glover, P. M.; McDonald, P. J.; Keddie, J. L.; Wallin, M.; Motiejauskaite, A.; Weissenborn, P. K. *J. Coat. Technol.* **2002**, *74*, 113−124.
(10) Hein, R. W. *J. Coat. Technol.* **1998**, *70*, 19−22.
(11) Hein, R. W. *J. Coat. Technol.* **1999**, *71*, 21−25.
(12) Schrof, W.; Beck, E.; Koniger, R.; Reich, W.; Schwalm, R. *Prog. Org. Coat.* **1999**, *35*, 197−204.
(13) Schrof, W.; Beck, E.; Etzrodt, G.; Hintze-Bruning, H.; Meisenburg, U.; Schwalm, R.; Warming, J. *Prog. Org. Coat.* **2001**, *43*, 1−9.
(14) Froud, C. A.; Hayward, I. P.; Laven, J. *Appl. Spectrosc.* **2003**, *57*, 1468−1474.
(15) Everall, N. J. *Appl. Spectrosc.* **2000**, *54*, 1515−1520.
(16) Everall, N. J. *J. Coat. Technol.* **2005**, *2*, 38−44.
(17) Everall, N. J. *J. Coat. Technol.* **2005**, *2*, 46−52.
(18) Glover, P. M.; Aptaker, P. S.; Bowler, J. R.; Ciampi, E.; McDonald, P. J. *J. Magn. Reson.* **1999**, *139*, 90−97.
(19) Hubert, J. C.; Venderbosch, R. A. M.; Muizebelt, W. J.; Klaasen, R. P.; Zabel, K. H. *Prog. Org. Coat.* **1997**, *31*, 331−340.
(20) Hubert, J. C.; Venderbosch, R. A. M.; Muizebelt, W. J.; Klaasen, R. P.; Zabel, K. H. *J. Coat. Technol.* **1997**, *69*, 59−64.
(21) Muizebelt, W. J.; Donkerbroek, J. J.; Nielen, M. W. F.; Hussem, J. B.; Biemond, M. E. F.; Klaasen, R. P.; Zabel, K. H. *J. Coat. Technol.* **1998**, *70*, 83−93.
(22) Muizebelt, W. J.; Hubert, J. C.; Nielen, M. W. F.; Klaasen, R. P.; Zabel, K. H. *Prog. Org. Coat.* **2000**, *40*, 121−130.
(23) Mallegol, J.; Gonon, L.; Commereuc, S.; Verney, V. *Prog. Org. Coat.* **2001**, *41*, 171−176.
(24) Mueller, E. R. *Ind. Eng. Chem.* **1954**, *46*, 562−569.
(25) van Gorkum, R.; Bouwman, E. *Coord. Chem. Rev.* **2005**, *249*, 1709−1728.
(26) Ostroff, E. D.; Waugh, J. S. *Phys. Rev. Lett.* **1966**, *16*, 1097−1098.
(27) Erich, S. J. F.; Laven, J.; Pel, L.; Huinink, H. P.; Kopinga, K. *Prog. Org. Coat.* **2005**, *52*, 210−216.
(28) Erich, S. J. F.; Laven, J.; Pel, L.; Huinink, H. P.; Kopinga, K. *Appl. Phys. Lett.* **2005**, *86*, 134105.